Journal of Solid State Chemistry **166,** 191–196 (2002)
doi:10.1006/jssc.2002.9581, available online at http://www.idealibrary.com on IDEAL®

Subsolidus Phase Equilibria in the System $CaO–Al_2O_3–CoO$ and the Crystal Structure of Novel $Ca_3CoAl_4O_{10}$

B. Vazquez,* L. M. Torres-Martinez,* N. Alvarez,† J. F. Vente,‡ and P. Quintana‡,[1]

*Facultad de Ciencias Quimicas, Universidad Autonoma de Nuevo Leon, A.P. 1864, Monterrey, Nuevo Leon, Mexico; †Universidad de la Habana, Zapata y G. Plaza de la Revolucion, Cd. de la Habana, Cuba; ‡Department of Applied Physics, CINVESTAV IPN-Unidad Merida, Km 6 Antigua Carretera a Progreso, Cordemex, C.P. 97310 Merida, Yucatan, Mexico

Received November 28, 2001; in revised form February 25, 2002; accepted March 8, 2002

The subsolidus phase diagram, $CaO–Al_2O_3–CoO$, and its phase relations below 1300°C have been studied in air. The stability regions of nine subsolidus compatibility triangles were established and a new ternary phase was found. The structure of this compound, $Ca_3CoAl_4O_{10}$ (orthorhombic, space group $Pbc2_1$, $a = 5.1452(2)$ Å, $b = 16.7731(5)$ Å, $c = 10.7055(3)$ Å), was determined from X-ray diffraction data and found to be isostructural with $Ca_3ZnAl_4O_{10}$. This is an open framework compound with three crystallographically different channels, each with a diameter of ~ 3.5 Å. The two end members of the binary CoO–CaO system are surrounded by small regions of solid solutions. Lab color parameters were measured in several compositions. No ternary phases were found when Co was substituted by other divalent cations such as Sr, Ba, Mn, Ni, Cu, Cd, Sn and Pb. © 2002 Elsevier Science (USA)

Key Words: **phase diagram; cobalt calcium-aluminates; X-ray diffraction; Rietveld analysis; color measurements.**

INTRODUCTION

Only a very limited number of studies has been performed on the ternary system $CaO–Al_2O_3–MO$. The driving force to study the system with $M = Mg$ is related to its geological occurrence and to processes in the ceramics industry (1–6). Several ternary compounds have been reported as $Ca_3MgAl_4O_{10}$, a metastable phase $Ca_7MgAl_{10}O_{23}$ (1, 5), and $Ca_2Mg_2Al_{28}O_{46}$ and $CaMg_2Al_{16}O_{27}$ in the alumina-rich part (6–8). The system with $M = Zn$ has also been studied to some extent (9), for its importance of stabilizing waste raw materials in cement. As ternary compounds, apart from $Ca_3ZnAl_4O_{10}$, $Ca_3Zn_3Al_4O_{15}$ and $Ca_{14}Zn_6Al_{10}O_{35}$, have also been reported (9, 10).

As part of our ongoing research into the phase relations of concrete and cement-related materials and its possible application for the safe and stable disposal of raw-related materials, we have studied the system $CaO–Al_2O_3–CoO$. Mixtures of cobalt-rich oxides, with aluminum and/or silicon oxides as additives are widely used for colored glazes in the ceramic industry. In the glass industry, it is applied to create blue hues and to mask the greenish tinge of glass and porcelain caused by iron impurities (11, 12). These compounds are characterized by having a high stability with respect to light, environment, high temperature and chemicals (13, 14).

The three limiting two-component diagrams in the ternary system $CaO–Al_2O_3–CoO$ are well established and contain a number of binary phases. In the $CaO–Al_2O_3$ system, several binary compounds have been reported (15, 16): $Ca_3Al_2O_6$, $Ca_{12}Al_{14}O_{33}$, $CaAl_2O_4$, $CaAl_4O_7$ and $CaAl_6O_{10}$. However, the presence of moisture has a great influence on the formation and the stability of $Ca_{12}Al_{14}O_{33}$ (C12A7) (7, 16, 17). The only compound found in the system $CoO–Al_2O_3$ is $CoAl_2O_4$ (18). No compound with the general formula $Ca_{1-x}Co_xO$ is known. However, CaO and CoO do react and form at least four different compounds in which cobalt has a higher formal valence (19, 20). More recently, $Ca_3Co_2O_6$ has attracted some attention for its one-dimensional properties (21, 22) and $Ca_3Co_4O_9$ for its anisotropic giant magnetoresistance (23). However, the average formal valence of cobalt in these compounds is three.

In this paper, the phase diagram of the ternary system $CaO–Al_2O_3–CoO$ and a description of the new ternary phase $Ca_3CoAl_4O_{10}$ are presented. Unsuccessful attempts were made to synthesize other ternary compounds replacing CoO by MO, with M = Sr, Ba, Mn, Ni, Cu, Cd, Sn and Pb.

EXPERIMENTAL

In order to determine the phase diagram $CaO–Al_2O_3–CoO$, over 50 strategically chosen compositions were prepared by traditional solid-state techniques, using high-purity (> 99.99%), $CaCO_3$, Al_2O_3 and CoO. Appropriate amounts of the dried reagents were mixed in acetone until

[1] To whom corresponence should be addressed. Fax: + 52-999-9812917. E-mail: pquint@mda.cinvestav.mx.

0022-4596/02 $35.00

all the acetone had evaporated (~ 10 min). The mixtures thus formed were preheated at ~ 700°C for a few hours to allow the carbonate to dissociate. Subsequently, the mixtures were reground, pelletized and heated at temperatures up to a maximum of 1300°C for a period of 2–15 days, depending on the composition. The reactions were regularly interrupted to allow for regrinding and repelletizing and to measure the X-ray diffraction pattern at room temperature. The reactions were terminated when either a single phase had been formed or when subsequent X-ray diffraction patterns did not show any indication of an ongoing reaction. All reactions were performed in Pt crucibles under air. Similar procedures were followed for the systems $CaO–Al_2O_3–M^{2+}O$, with M^{2+} = Sr, Ba, Mn, Ni, Cu, Cd, Sn and Pb.

To obtain a pure sample of the new ternary phase $Ca_3CoAl_4O_{10}$, it was necessary to grind the reaction mixture in acetone for an extended period of time (40 min), during the early stages of heating, to promote the contact and favor the reaction between the reagents. Subsequently, the mixture was heated at 900°C for a period of 12 h to drive off CO_2. The powder was reground and pressed into pellets. The pellets were heated, increasing the temperature with intervals of 50°C every 24 h up to 1200°C. The sample was annealed at this temperature for 15 days, the reaction was frequently interrupted to allow additional grinding and repelletizing.

Room-temperature diffraction data were collected in the angular range $8 \leq 2\theta/^\circ \leq 100$ in steps of 0.02° 2θ, with a counting time of 15 *s* per step, using a Siemens D-5000 diffractometer, operating with $CuK\alpha_{1+2}$ radiation in Bragg–Brentano geometry. The diffraction pattern of the newly found compound $Ca_3CoAl_4O_{10}$ was analyzed by Rietveld refinement (24) using the GSAS suite of programs (25). The background level was fitted using a 6-term shifted Chebyshev polynomial and the peak shapes were described with a pseudo-Voigt function. The Bragg reflection with the highest intensity (113) located at $\sim 30.9^\circ$ 2θ was individually fitted to two identical pseudo-Voigt functions, with a fixed intensity ratio of 0.5, and separated according to the ratio of the wavelengths of the $CuK\alpha_1$ and $CuK\alpha_2$ radiations.

The color of selected samples was determined in L*a*b* color space, using diffuse reflectance UV–V spectroscopy in the range $360 \leq \lambda/\text{nm} \leq 750$ with a Macbeth CE-7000^a spectrometer. Measurements were made with a light source D65 and a 10° observer. The L*a*b* coordinates give the parameters of the color in a specific position in a three-dimensional CIELAB color space (26), that is based on the Commission International de l'Eclairage (CIE) system. The lightness and saturation (the deviation from gray) are evaluated by L*, the terms a* and b* determine the hue of a material and defines whether the color tends to red/green or to yellow/blue, respectively.

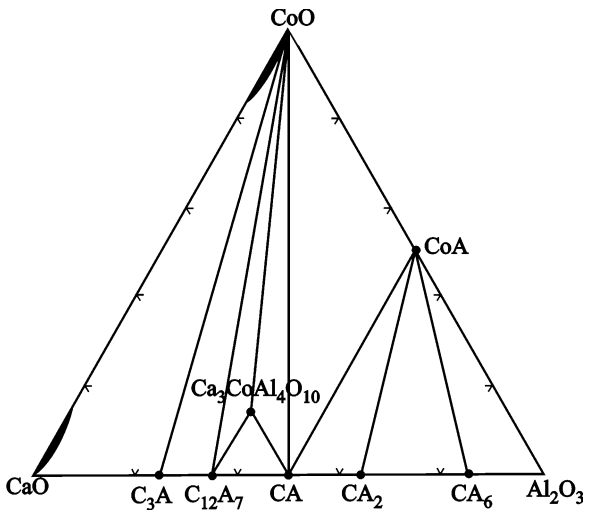

FIG. 1. Subsolidus phase diagrams $CaO–Al_2O_3–CoO$ studied in air atmosphere at a maximum temperature of 1300°C.

RESULTS

The ternary phase diagram constructed for the system $CaO–Al_2O_3–CoO$, based on the experiments described above is shown in Fig. 1. The phase triangle does not show many features and the only ternary phase present is $Ca_3CoAl_4O_{10}$. Solid solutions are present in two separate regions, represented as shaded areas in Fig. 1. These regions can be found near the end members of the binary phase diagram, CaO–CoO. Relatively small amounts of Ca (Co) can dissolve in CoO (CaO). A limited amount of Al can dissolve in the formed solid solutions, but not in either of the pure phases, CaO or CoO. No attempts have been made to determine the solubility limits of these solid solutions, and the regions drawn in Fig. 1 are based on the phase diagram reported by Woermann and Muan (20).

The ternary phase $Ca_3CoAl_4O_{10}$ forms rather slowly and it was difficult to prepare without any impurities, thus, hindering the determination of its composition. The low reaction rate is due to the initial formation of mayenite, $Ca_{12}Al_{14}O_{33}$. This compound forms very rapidly, often under non-equilibrium conditions, and once formed, the reaction continues very slowly. The appearance of mayenite is favored by the presence of a small amount of water, less than 1% mass (gained by grinding the mixture in air) and humidity, and $Ca_{12}Al_{14}O_{33}$ melts (17) around 1400°C. The reaction could not be forced by using a higher temperature than the one used, 1200°C, as $Ca_3CoAl_4O_{10}$ has a relatively low melting point (~ 1250°C). The composition of this phase was determined after performing a number of reactions with compositions in this region of the phase diagram with a prolonged heating time. Finally, a 2 g batch of pure $Ca_3CoAl_4O_{10}$ was obtained.

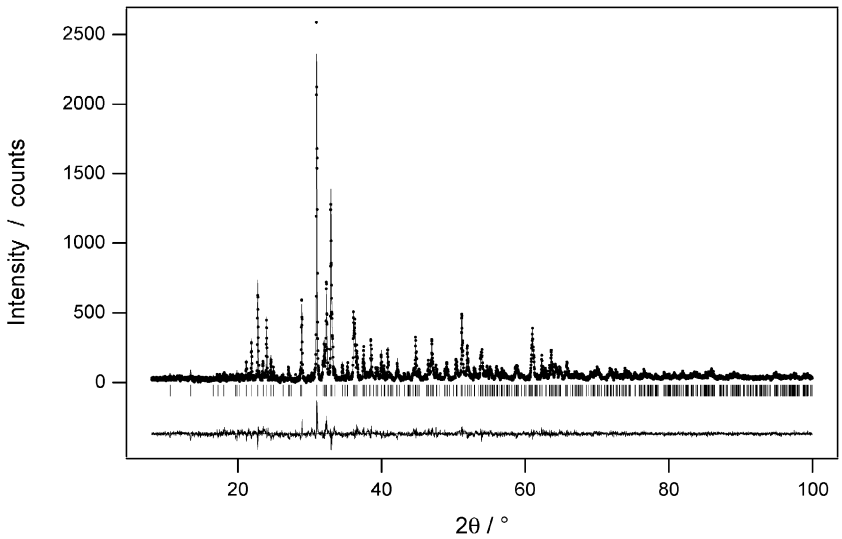

FIG. 2. Observed and difference XRD profile for $Ca_3CoAl_4O_{10}$.

The diffraction pattern of $Ca_3CoAl_4O_{10}$ appeared to be very similar to that of $Ca_3ZnAl_4O_{10}$ (10), and it could be indexed on the basis of an orthorhombic cell with parameters $a \sim 5.15$ Å, $b \sim 16.77$ Å, $c \sim 10.70$ Å. The reflection conditions were consistent with space group $Pbc2_1$, and we took the structure of $Ca_3ZnAl_4O_{10}$ (10) as a trial model. However, a full-matrix least-squares refinement including all common variables in an unconstrained manner, resulted in an unstable refinement and unrealistically short cation–oxygen distances. This reflects the complexity of this refinement and indicates that a large number of parameters (53) are required to describe the atomic positions. However, we were able to obtain a self-consistent model by applying soft constraints to the Al–O and Co–O bond distances. The average Al–O bond distance in $Ca_3ZnAl_4O_{10}$ (1.77 Å) was applied with a standard deviation of 0.02 Å. Several bond distances were tried for Co–O, the best fit was achieved with a value of 2.00 Å with a standard deviation of 0.01 Å. This distance is consistent with the effective ionic radii (27) of tetrahedrally coordinated Co^{2+} and O^{2-}. The weight factor was initially set to a high value and reduced in subsequent refinements. The minimum value applied (FACTR = 1) allowed a maximum freedom in O coordinates. Further

TABLE 1
Structural Parameters of $Ca_3CoAl_4O_{10}$ (e.s.d. in Parentheses)

Atom	x	y	z	U_{iso}
Ca(1)	0.290(2)	−0.1106(8)	0.6545(8)	0.013(2)
Ca(2)	0.319(2)	−0.1061(8)	0	
Ca(3)	0.712(1)	0.2073(3)	0.837(2)	
Co	0.126(2)	0.0750(5)	0.673(2)	0.016(1)
Al(1)	−0.368(2)	0.0308(6)	0.833(2)	0.017(1)
Al(2)	0.749(2)	−0.1662(6)	0.825(3)	
Al(3)	0.195(2)	0.254(2)	0.578(3)	
Al(4)	0.141(4)	0.084(1)	0.973(2)	
O(1)	0.082(3)	0.663(1)	0.321(4)	0.001(2)
O(2)	0.410(3)	0.4267(9)	0.839(3)	
O(3)	0.955(2)	0.455(1)	0.339(1)	
O(4)	0.405(5)	0.288(2)	0.692(2)	
O(5)	0.025(6)	0.488(1)	0.572(2)	
O(6)	−0.007(6)	0.325(1)	0.513(3)	
O(7)	0.484(4)	0.427(2)	0.475(2)	
O(8)	0.390(5)	0.278(2)	0.651(2)	
O(9)	−0.023(5)	0.316(1)	0.135(3)	
O(10)	0.502(3)	0.414(1)	0.213(2)	

Note. Space group $Pbc2_1$, $a = 5.1452(2)$ Å, $b = 16.7731(5)$ Å, $c = 10.7054(3)$ Å, $V = 923.88(6)$ Å, $R_{wp} = 14.07\%$, $R_p = 10.98\%$, $\chi^2 = 1.70$ for 70 variables.

TABLE 2
Interatomic Distances of $Ca_3CoAl_4O_{10}$ (Å)

Distances					
Ca(1)–O(1)	2.26(4)	Ca(2)–O(1)	2.46(4)	Ca(3)–O(1)	2.42(1)
Ca(1)–O(2)	2.58(4)	Ca(2)–O(2)	2.28(3)	Ca(3)–O(3)	3.00(2)
Ca(1)–O(4)	2.35(3)	Ca(2)–O(5)	2.59(3)	Ca(3)–O(4)	2.60(3)
Ca(1)–O(5)	2.48(3)	Ca(2)–O(8)	2.50(3)	Ca(3)–O(6)	2.43(3)
Ca(1)–O(6)	2.36(3)	Ca(2)–O(9)	2.46(4)	Ca(3)–O(7)	2.93(3)
Ca(1)–O(7)	2.33(3)	Ca(2)–O(10)	2.49(3)	Ca(3)–O(8)	2.38(3)
Mean	2.39	Mean	2.46	Ca(3)–O(9)	2.58(3)
				Ca(3)–O(10)	2.67(3)
Al(1)–O(2)	1.76(1)	Al(3)–O(4)	1.73(2)	Mean	2.63
Al(1)–O(3)	1.68(2)	Al(3)–O(6)	1.73(2)		
Al(1)–O(7)	1.84(2)	Al(3)–O(8)	1.77(2)	Co–O(3)	2.05(1)
Al(1)–O(10)	1.71(2)	Al(3)–O(9)	1.74(2)	Co–O(5)	1.96(1)
Al(2)–O(1)	1.71(1)	Al(4)–O(3)	1.85(2)	Co–O(9)	2.01(1)
Al(2)–O(2)	1.77(1)	Al(4)–O(5)	1.71(2)	Co–O(10)	1.99(1)
Al(2)–O(4)	1.80(2)	Al(4)–O(6)	1.77(2)		
Al(2)–O(8)	1.79(2)	Al(4)–O(7)	1.77(2)	O(3)–O(5)	2.58(3)

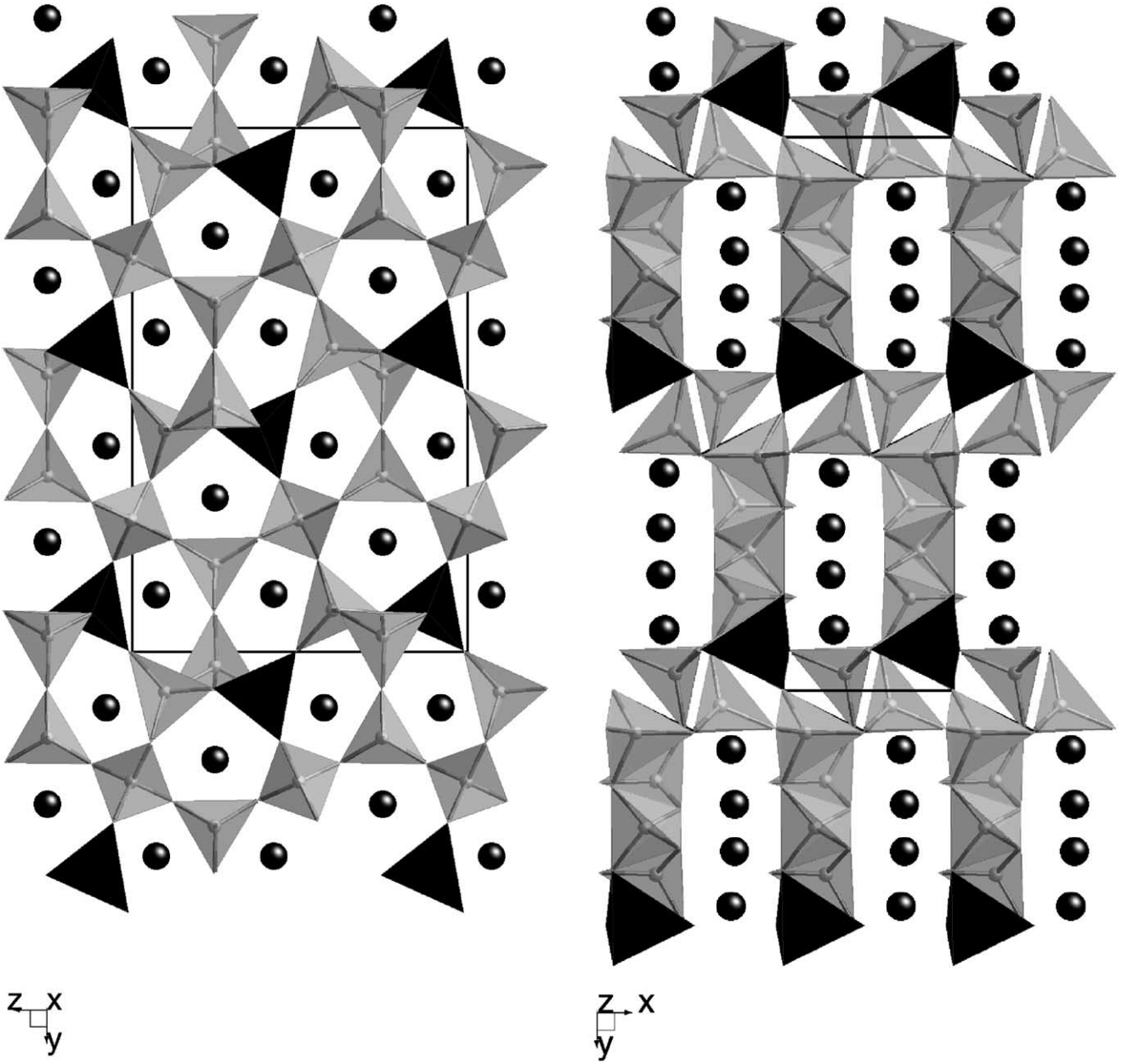

FIG. 3. The crystal structure of $Ca_3CoAl_4O_{10}$ showing the framework formed by CoO_4 (dark) and AlO_4 (light) tetrahedra and the calcium ions as black circles, viewed along (a) [100]; (b) [001].

reduction did not result in improved fit parameters. The large number of parameters also led to a reduction in the number of isotropic thermal factors that could be used; four were assigned: one for each Ca, Co, Al and O. The diffraction profiles are shown in Fig. 2, the refined structural parameters are given in Table 1 and a list of selected bond distances is presented in Table 2. We omit bond angles from this table to emphasize the limitations of our structural model. The refined structural model, viewed along [100] and [001], is shown in Figs 3a and 3b, respectively. The width of the pseudo-Voigt peaks used to fit the (113) reflections was found to be $\sim 0.08^\circ$ 2θ, close to the instrumental values, indicating a high degree of crystallinity.

The different compositions present in the current phase diagram show a wide range of different colors. The CaO-rich end is light gray, that turns to an olive green on doping with small quantities of CoO and Al_2O_3. The compositions in a wide central part of the diagram are deeply black, that extends to CoO end. The color of the compositions towards the Al_2O_3-rich end showed a variety of intense blue hues, as often observed for cobalt-containing compounds. The quantified color values of some selected Co-poor samples,

TABLE 3
Lab Color Values for Some Compositions in the System $CaO–CoO–Al_2O_3$

Sample no.	% Molar composition			Color parameters		
	CaO	Al_2O_3	CoO	L^a	a^a	b^a
1[a]	50.0	33.3	16.7	41.323	− 1.662	− 1.954
2	34.3	40.0	25.7	54.199	− 5.169	0.276
3	30.0	50.0	20.0	48.189	− 8.279	− 13.891
4	20.0	65.0	15.0	56.535	2.588	− 31.453
5	60.0	15.0	25.0	50.205	− 1.515	5.798
6	90.0	05.0	05.0	67.426	− 1.056	12.029
7	94.0	03.0	03.0	74.386	− 3.059	1.134

[a] $Ca_3CoAl_4O_{10}$.

expressed in the space–color L*a*b* coordinates, are given in Table 3. The variation on the saturation is a dark gray, since all L* values are near 50%, except for compositions near CaO, which shows a strong tendency to the white region. The hue presents a strong dark color except for composition No. 6 that shows a trend towards the yellow region and the rich-alumina composition (No. 4) to the blue region.

DISCUSSION

The phase diagram as determined is straight forward. The bordering compositions of the compatibility triangles are mainly binary compounds as found on the edges of the overall subsolidus phase diagram. In the binary $CaO–Al_2O_3$ system, mayenite (C12A7) was considered in the diagram, even so it is known that it is not stable under strictly anhydrous conditions but is stabilized by the presence of moisture, even at high temperatures (5, 7, 17). The diagram was not studied in an absolutely moisture-free atmosphere, i.e., air, and since the reactions were interrupted repeatedly for additional grindings, it is believed that water was present and mayenite should be considered to be stable under the present conditions. The solid solubilities of CaOss and CoOss end members extend into the ternary diagram, and it is often observed together with $Ca_3Al_2O_6$. The existence of this type of solid solution was deducted from the behavior of the cell parameters of the phases present in multiphase mixtures with a composition outside the regions of the solid solutions. The solubility limits in the ternary diagram were not determined but they are consistent with other similar systems such as $CaO–Al_2O_3–M^{2+}O$ with M = Mg (5) and Ni (28).

The refinement of the crystal structure of the only ternary compound present in this phase diagram, $Ca_3CoAl_4O_{10}$, was troublesome due to the large amount of positional parameters. We were forced to use soft constraints on some of the cation–oxide bond distances, to prevent the refinement from diverging and to prevent the occurrence of unrealistic Al–O and Co–O distances. The structural determination was especially insensitive to the positions of the lightest atom present in the structure: oxygen. The bond distances used in the soft constraint were consistent with the well-established ionic radii (27) of Co^{2+}, Al^{3+} and O^{2-}. The mean Ca–O bond distances, which were unconstrained, are in perfect agreement with those presented for $Ca_3ZnAl_4O_{10}$ (10), and the shortest O–O contact (2.58(3) Å) is chemically sensible. We therefore conclude that $Ca_3CoAl_4CoO_{10}$ is isostructural with $Ca_3ZnAl_4ZnO_{10}$, despite the fact that the mean Co^{2+}–O distance (2.00 Å) is significantly larger than the mean Zn^{2+}–O distance (1.83 Å). The concomitant change in volume of $\sim 0.1\%$ is achieved in an anisotropic manner, with the expansion in the *b*-parameter being the largest ($\sim 0.1\%$). The *a*- and *c*- parameters remain virtually unchanged, with changes smaller than 0.05% or 0.004 Å. This structure has been described before (10). Three crystallographic distinct channels run parallel with [100] and each is occupied by only one Ca cation (Fig. 3a). Two of these channels are very similar and contain Ca(1) and Ca(2) both in octahedral coordination with an average Ca–O distance of 2.39 and 2.46 Å, respectively. Five-membered rings of tetrahedra run around these channels which measure ~ 2.9 Å by ~ 4.1 Å. The significantly larger third channel (~ 3.5 Å by ~ 4.1 Å) contains Ca(3) an irregular eight-coordination with an average Ca–O distance of 2.63 Å. This channel which is again bordered by five tetrahedra, appears more circular than the other two. Perpendicular to these three channels, a rectangular channel is observed (~ 5.9 Å by ~ 2.9 Å), which contain all three calcium ions (Fig. 3b). These channels are bordered by eight tetrahedra.

ACKNOWLEDGMENTS

B. Vazquez thanks Conacyt for a fellowship (118729-120447). P. Quintana kindly acknowledges CONACYT for the financial support for the Catedra Patrimonial de Excelencia Nivel II (970030-R98). We are indebted to L. Rendon at Instituto de Fisica, UNAM for experimental assistance.

REFERENCES

1. J. H. Welch, *Nature* **191,** 559 (1961).
2. A. J. Majumdar, *Trans. Br. Ceram. Soc.* **63,** 347 (1964).
3. A. J. Majumdar, *J. Am. Ceram. Soc.* **64,** 416 (1965).
4. F. P. Glasser and J. Marr, *Trans. Br. Ceram. Soc.* **74,** 113 (1975).
5. B. Hallstedt, *J. Am. Ceram. Soc.* **78,** 193 (1995).
6. M. Göbbels, E. Woermann, and J. Jung, *J. Solid State Chem.* **120,** 358 (1995).
7. A. H. De Aza, P. Pena, and S. De Aza, *J. Am. Ceram. Soc.* **82,** 2193 (1999).
8. A. H. De Aza, J. E. Iglesias, P. Pena, and S. De Aza, *J. Am. Ceram. Soc.* **83,** 919 (2000).
9. H. Bolio-Arceo and F. P. Glasser, *J. Adv. Cem. Res.* **10,** 25 (1998).

10. V. D. Barbanyagre, T. I. Timoshenko, A. M. Ilyinets, and V. M. Shamshurov, *Powder Diffract*. **12,** 22 (1997).
11. R. K. Mason, *Ceram. Bull.* **40,** 5 (1961).
12. J. Alarcon, P. Escribano, and R. Ma. Marin, *Trans. Br. Ceram. Soc*. **84,** 170 (1985).
13. S. Djambazov, I. Ivanova, A. Yoleva, and N. Nedelchev, *Ceram. Int*. **24,** 281 (1998)
14. F. Singer and S. S. Singer, "Industrial Ceramics." Chapman & Hall, Ltd, London, 1963.
15. R. W. Nurse, J. H. Welch, and A. J. Majumdar, *Trans. Br. Ceram. Soc*. **64,** 323 (1965).
16. B. Hallstedt, *J. Am. Ceram. Soc*. **73,** 15 (1990).
17. D. A. Jerebtsov and G. G. Mikhailov, *Ceram. Int*. **27,** 25 (2001).
18. T. Mori, *Yogro Kyokaishi* **90,** 100 (1982).
19. C. Brisi and P. Rolando, *Ann. Chim.* **58,** 681 (1968).
20. E. Woermann and A. Muan, *J. Inorg. Nucl. Chem.* **32,** 1457 (1970).
21. H. Fjellvåg, E. Gulbrandsen, S. Aasland, A. Olsen, and B. C. Hauback, *J. Solid State Chem.* **124,** 190 (1996).
22. S. Aasland, H. Fjellvåg, and B. Hauback, *Solid State Commun.* **101,** 187 (1997).
23. A. C. Masset, C. Michel, A. Maignan, M. Hervieu, O. Toulemonde, F. Studer, B. Raveau, and J. Hejtmanek, *Phys. Rev*. **62,** 166 (2000).
24. H. M. Rietveld, *J. Appl. Crystallogr*. **2,** 65 (1969).
25. A. C. Larson and R. B. von-Dreele, "General Structure Analysis System (GSAS)." Los Alamos National Laboratories, Report LAUR 86-748 (1990).
26. ASTM- E: 308-80, "Standard Test Method for Computing the Colours of Objects by Using the CIE System," February, 1991.
27. R. D. Shannon, *Acta Crystallogr. A* **32,** 519 (1976).
28. P. Lopez-Armandariz, "Efecto de la incorporación de niquel en el clinker del cemento." M.Sc. Thesis in Ceramic Engineering, UANL, October, 1997.